

# Polyamide 12 modified with nanoparticles: Effect on impact behaviour and on the electrical conductivity of carbon fibre-reinforced epoxy composites

Marcus Arnold<sup>1</sup>, Markus Henne<sup>1</sup>, Klaus Bender<sup>2</sup> and Klaus Drechsler<sup>3</sup>

## Abstract

Modifying the impact toughness of carbon composite by means of introducing thermoplastic inserts in the interlaminar layer is state of the art. However, these inlayers reduce the electrical conductivity through the thickness of the composite. Because the combination of good electrical conductivity and high fracture toughness is desirable, a detailed investigation was carried out into additive-enhanced polyamide 12 compound. The modification consisted in compounding graphite, graphene and carbon nanotubes with polyamide 12 in various proportions. After it was introduced into the interlaminar layer, the samples' electrical conductivity was measured and their mechanical properties assessed. Afterwards, these results were compared with various inserts made with unmodified polyamide 12. It turned out that the coarse-mesh laid scrim showed only a slight fall in conductivity. Furthermore, it provided promising results regarding the increase of the interlaminar toughness. Thus, the expensive modification of polyamide 12 can be avoided by using discrete laid scrim.

## Keywords

Carbon fibre-reinforced plastics, interlaminar fracture toughness, polyamide 12, laid scrim, electrical conductivity, mechanical properties

## Introduction

At this time, a stepwise change is taking place in the aircraft industry from structures made of metal to those made of composites. The latest types of wide-bodied aircraft, such as the Airbus A380 and A350, and the Boeing 787, are made to a large extent using fibre-reinforced composites, often of carbon fibres in a matrix of epoxy resin. Carbon composites combine light weight with great strength and stiffness, but are brittle when exposed to impact loading (e.g. hail strike, bird strike, tool dropping), which can cause severe damage to the component.<sup>1,2</sup> Various studies have been concerned with increasing fracture toughness, for which an effective method is to introduce a thermoplastic material, the so-called inlayer, into the interlaminar layer.<sup>3,4</sup>

Lightning strike is a phenomenon that occurs regularly in aviation: the statistics show that an aircraft is hit by lightning once every 3000 flying hours, which for

commercial aircraft means once a year.<sup>5</sup> The strike gives rise to a high-intensity electrical current which flows through those components having the lowest electrical resistance. Should the surface skin of the aircraft not be well enough protected, this current can have serious consequences such as vaporizing metal parts, control lines or other critical components.<sup>6</sup> Metallic

<sup>1</sup>University of Applied Sciences Rapperswil, Institute of Material Science and Plastics Processing, Rapperswil, Switzerland

<sup>2</sup>EMS-CHEMIE AG, Business Unit EMS-GRILTECH, Domat/Ems, Switzerland

<sup>3</sup>Technische Universität München, Institute for Carbon Composites, Garching, Germany

### Corresponding author:

Markus Henne, Institute of Material Science and Plastics Processing, University of Applied Sciences Rapperswil, Oberseestrasse 10, CH-8640 Rapperswil, Switzerland.  
Email: mhenne@hsr.ch

aircraft structures, which often are of aluminium, withstand lightning strikes without damage because they can easily lead away over the outer skin of the aircraft the heavy currents that result from a strike.<sup>7,8</sup>

In order to protect modern commercial aircraft against lightning strikes despite the low electrical conductivity of carbon fibre reinforced plastics (CFRP), the electrical conductivity of the latter is typically increased by means of a metallic insert in the outermost layer.<sup>9</sup> Various alternative approaches are being investigated, for example increasing their conductivity by adding electrically conducting nanoparticles.<sup>10,11</sup> However, protecting CFRP against lightning is very complex because the high electrical resistance of the epoxy resin between the carbon fibre layers, together with the anisotropic nature of the composite structure, makes them poor conductors of electricity. CFRP has about 2000 times the electrical resistance of aluminium. Epoxy resin, with a resistance a million times that of aluminium, belongs to the class of insulating materials.<sup>5</sup>

For this reason, the heavy currents resulting from lightning strikes cannot be efficiently led away over an outer skin made of carbon fibre composites in order to prevent damage to the airframe. A lightning strike can cause damage to the surface skin such as embrittlement of the matrix or delamination, and thus lead to damage to the structure.<sup>12–15</sup> In addition, the heavy current can penetrate to parts of the airframe itself, such as the ribs and spars. At connections between components, the so-called “edge glow effect” can occur, which leads to voltage differences between structural components that are high enough to cause sparks or electric arcing.<sup>16</sup> It is therefore particularly important to avoid edge-glow in the neighbourhood of the fuel tanks, for example in the wing boxes.

Thermoplastic inlayers can further intensify this effect. Placing inlayers strengthens the electrical insulation between the individual fibre layers. This manifests itself in reduced conductivity, especially in the direction of the thickness.<sup>17</sup> A lightning strike causes a strong electrical field to form between the insulated layers, producing a flow of electrons over the fibre layers toward the edges of the component which can in turn lead to arcing.<sup>18</sup> For this reason, it is desirable to combine increased fracture toughness with improved electrical conductivity.

This study contains a detailed comparison of the way variously modified polyamide 12 (PA12), introduced into the interlaminar layer of CFRP, affects its electrical and mechanical properties. For this purpose, graphite, graphene and carbon nanotubes were severally mixed in various proportions with PA12 powder. Table 1 gives the respective proportions and standard particle sizes. To determine the influence of the semi-finished product on the mechanical and electrical properties, additional CFRP samples were modified with a

continuous non-woven fabric (NWF) as well as two different discrete laid scrims and their results compared with the other samples. Although the electrical and mechanical characteristics of these materials differ significantly, each of them offers good potential for modifying the properties of the resulting composite.

## Materials and details of the experiments

### Materials

The reinforcing fibres of the epoxy laminates consisted of a unidirectional carbon fibre web with a specific weight of 298 g/m<sup>2</sup>. This web was based on Toho Tenax® J IMS60 E13 fibres and was supplied by SAERTEX GmbH & Co. KG. The single-component resin system HEXFLOW RTM 6 (RTM6) was used, supplied by Hexcel. These materials were used as supplied.

Ovation Polymers Inc. delivered the master batch of graphene, with a 15% graphene content by weight, and EMS-CHEMIE AG the master batch of carbon nanotubes (CNT) with 20% CNT by weight. Since there was no corresponding master batch of graphite available, they were manufactured in-house. Timcal AG supplied the C-Therm 001 graphite powder, which was compounded with PA12 in a Coperion ZSK 26 co-rotating twin screw extruder into granules with, respectively, 10%, 20% and 30% graphite content by weight. EMS-CHEMIE AG then converted all the granulates into powder by means of a cryogenic grinder, finally sifting the powder to a grain size of 0–80 µm.

In order to set the test results more in context, the range of materials tested was expanded to include PA12 inserts in the form of NWF at a specific weight of 19 g/m<sup>2</sup> and laid scrims of differing specific weights and mesh spacing. Laid scrim 1 was of 300 dtex yarn with warp spacing 5.5 mm and weft spacing 13 mm, giving a specific weight of 12 g/m<sup>2</sup>. Laid scrim 2 on the other hand consisted of 75 dtex yarn with warp spacing 1.4 mm and weft spacing 14 mm, giving a specific weight of 10 g/m<sup>2</sup>. The PA12 used to modify the fracture toughness was supplied by EMS-GRILTECH in the form of powder, as NWF and as yarn. BAFATEX Bellingroth GmbH & Co. KG used this yarn to fabricate the two laid scrims described earlier.

PA 12 was selected as a modifier since it will not melt during resin infusion or dissolves in the resin. The melting of the polymer, which is desired due to an increase of the adhesion area, does not occur until shortly before reaching the curing temperature of the resin.

### Producing the test samples

All the samples were produced by the Resin Transfer Infusion (RTI) process, in which the preforms are first

**Table 1.** Overview of the different interlayers, thickness and fibre volume content of the tested samples.

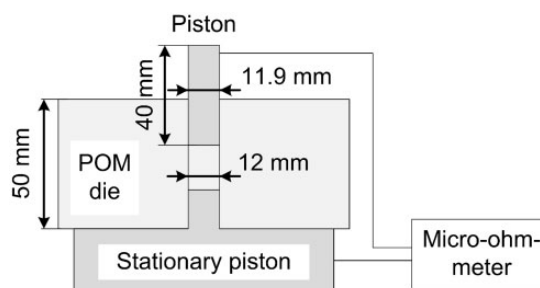
	Abbreviation	Interlayer		Lay up: [0/+45/-45/90] <sub>2S</sub>		Lay up: [0] <sub>10</sub>	
		Interlayer weight (g/m <sup>2</sup> )	Standard particle size (μm)	Thickness (mm)	Volume fraction	Thickness (mm)	Volume fraction
Reference	Ref	(-)	(-)	4.2	0.63	2.8	0.60
PA12 unmodified	PA12 UM	12	0-100	4.7	0.56	3.0	0.55
PA12 + Graphite (10 wt%)	G10	12	0-80	4.8	0.55	3.0	0.56
PA12 + Graphite (20 wt%)	G20	12	0-80	4.6	0.57	3.0	0.55
PA12 + Graphite (30 wt%)	G30	12	0-80	4.6	0.57	2.9	0.56
PA12 + Graphene (15 wt%)	Graphene	12	0-80	4.8	0.55	2.9	0.57
PA12 + CNT (20 wt%)	CNT	12	0-80	4.9	0.54	3.1	0.53
PA 12 non-woven fabric	NWF	19	(-)	5.1	0.52	3.3	0.51
PA12 laid scrim 1 (300dtex)	Laid scrim 1	12	(-)	4.9	0.54	3.3	0.51
PA12 laid scrim 2 (75 dtex)	Laid scrim 2	10	(-)	4.8	0.56	3.0	0.56

wetted with the epoxy resin by infusion and then cured in an autoclave. A steel plate coated with the release agent Frekote 770-NC served as the tool. The resin was preheated to 80 °C and the tool to 120 °C. The laminates for the CAI and ILSS tests were laid up in 16 layers in the quasi-isotropic pattern [0/+45/-45/90]<sub>2S</sub>, while those for the GIc, GIIC tests were formed in 10 layers in the [0]<sub>10</sub> pattern. All were cut into 330 × 330 mm samples. A fine-meshed sieve was used to spread the various powders uniformly to 12 g/m<sup>2</sup> in every interlaminar layer, while the laid scrims and the NWF were placed in between every two NCF in the course of building up the preforms.

After the assembly had been completely soaked by means of infusion, it was placed in the autoclave, which was then evacuated and heated up to 120 °C at 1.5 °C/minute and held at that temperature for 90 minutes, after which the pressure inside the autoclave was raised to 60 kPa. The temperature was then raised to 180 °C at the same rate of 1.5 °C/min, held at this level for 90 min, and then slowly reduced to ambient temperature. All the resulting composite laminated samples were tested according to the AITM 1-0010 standard, for porosity, homogeneity, and delamination. This was done by means of ultrasonic scanning using the Olympus OmniScan MX2 with the phased-array test head. All the samples were then cut out of the composite laminates with a Mutronic DIADISC 5200 water-cooled diamond saw.

### Determining the electrical conductivity of the modified powder

The electrical conductivity of graphite, graphene and CNT in powder form has been investigated in various studies,<sup>19-21</sup> in which it was found that the amount of powder used and the compressive force exerted had a decisive effect on the results.

**Figure 1.** Schematic view of the test rig used for determining the electrical conductivity of the various modified PA12 powders.

Tests on the variously modified PA12 have shown that a reproducible measurement of conductivity can be had using 0.1 g of powder. Tests under pressure were carried out according to the conditions specified in reference.<sup>20</sup> Figure 1 illustrates schematically the test rig that was used to do this. The body of the rig is a solid die made of Polyoxymethylene (POM) with an inner diameter of 12 mm, which is fixed in a vertical position on a cylindrical mount of copper having a coaxial fixed piston 11.9 mm in diameter and 15 mm long. A copper piston 11.9 mm in diameter and 40 mm long closes the die. In order to ensure good electrical contact between the test sample and the faces of the fixed and moving pistons, the latter are finely polished. The test rig is mounted in a Shimadzu AG-10kNX universal mechanical testing machine. After the cavity is filled with 0.100 ± 0.001 g of powder, the moving piston is lowered to increase the pressure on the powder from 0.25 MPa to 50 MPa, the piston position giving a measure of the thickness of the compressed powder.

The electrical resistance of the compressed powder was determined with a SEFELEC MGR10 micro-ohm meter using the Kelvin four-conductor principle, in which two conductors supply a DC current of between 0.1 mA and 10 A while the other two give the voltage

drop across the sample, so eliminating the potential error from the resistance of the current-carrying conductors. The measurements were made on five samples of each variant of powder.

### Determining the electrical conductivity of the composites

Investigations have shown that the sample dimensions can have a decisive influence on the measurement of electrical conductivity.<sup>22</sup> Samples of different sizes taken from the same laminate and given the same surface treatment can give differing results. Differences in the structures of samples with the same inter-fibre distance also contribute to such differing results. Micro short-circuits due to fractional contact between adjacent layers of fibre can also strongly affect the results. In order to master this situation, the electrical conductivities of five samples cut from the same laminate were measured. The laminates were of 10 layers with a  $[0]_{10}$  layup, this unidirectional layup being chosen because of the differences in material properties along the respective main axes of the composites. This made it possible to evaluate whether the electrically conducting PA12 powder had a positive influence on the electrical conductivity of the composites along the three main axes. Figure 2 identifies the three axes relative to the fibre direction.

Along with the geometry of the samples, the nature of the contact between the sample and the measuring device plays a decisive role. Studies have shown that appropriate treatment of the surface is necessary in order to ensure reproducible measurements.<sup>21–24</sup> Besides coating it with nickel, the surface can also be treated with a conductive silver paste. Furthermore, the sample should be put under pressure during the measurement because discontinuous contact can distort the result. In order to ensure that the surface texture of the sample affected the result as little as possible, the surfaces were first smoothed with P150 and then P400 abrasive paper, after which they were cleaned with acetone and subsequently dried in a temperature chamber for an hour at 65°C. The contact surfaces were then treated with a suspension of silver in methyl isobutyl ketone (Acheson Electrodag 1415M). Figure 3 is

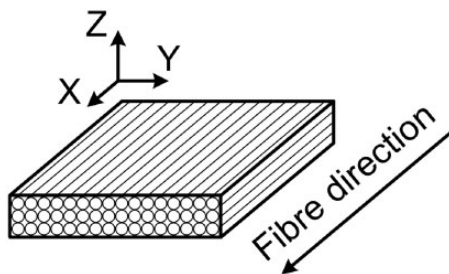


Figure 2. Identification of the main axes of the laminates.

a schematic view of the test rig. As with the compressed powder measurement, a SEFELEC MGR10 micro-ohm meter was used to determine the conductivity, with a test current of 10 mA DC.

In order to minimize the contact resistance while recording the test current and voltage drop, the sample was squeezed with a controlled pressure between solid copper electrodes in a Shimadzu AG-250kNX universal testing machine. Preliminary testing showed that in the *Y*-direction, increasing the pressure above 10 MPa brought no further improvement in the apparent electrical conductivity of a sample. However, in the *X*- and *Z*-directions, the pressure had to be increased to 50 MPa to achieve the same effect. For this reason, a testing pressure of 10 MPa was used for the measurements in the *Y*-direction and 50 MPa in the *X*- and *Z*-directions, respectively.

### Mechanical testing

The CAI samples measured 150 mm long by 100 mm wide. The impact loading of these samples, the subsequent measurement of the depth of the dent and the analysis of the damaged surface, as well as the compression test, were all in conformance with the Airbus AITM 1-0010 standard. The procedure was to clamp the sample to a heavy solid plate and to subject it to the impact of a 4.45 kg drop weight with a hemispherical nose 16 mm in diameter, an anti-rebound device ensuring that no second impact took place. The impact energy was 30 J throughout. After the depth of the dent was ascertained, the samples were again subjected to ultrasonic testing using the Olympus OmniScan MX2 with the phased-array test head, in which the delamination zone was defined using the half-value method and then quantified numerically and recorded. The compression testing was performed using a Shimadzu AG-250kNX materials testing machine with a constant test speed of 0.5 mm/min and standardized tooling. Five samples were produced and tested for each type of composite laminate.

The ILSS samples were cut from the laminates to a width of 9 mm and a length of 27 mm. The ILSS was carried out according to the ASTM D2344 standard using the Shimadzu AG-X 10kN universal testing machine and a standardized fixture supplied by Wyoming Test Fixtures. The distance between the cylindrical supports was 18 mm, resulting in a span-to-thickness ratio of about 4. A constant crosshead speed of 1 mm/min was used. The resulting short-beam strength can be evaluated by the following equation

$$F_{sbs} = 3P_m/4bh \quad (1)$$

with  $P_m$  = force at rupture,  $b$  = sample width and  $h$  = sample thickness. The effect on the interlaminar

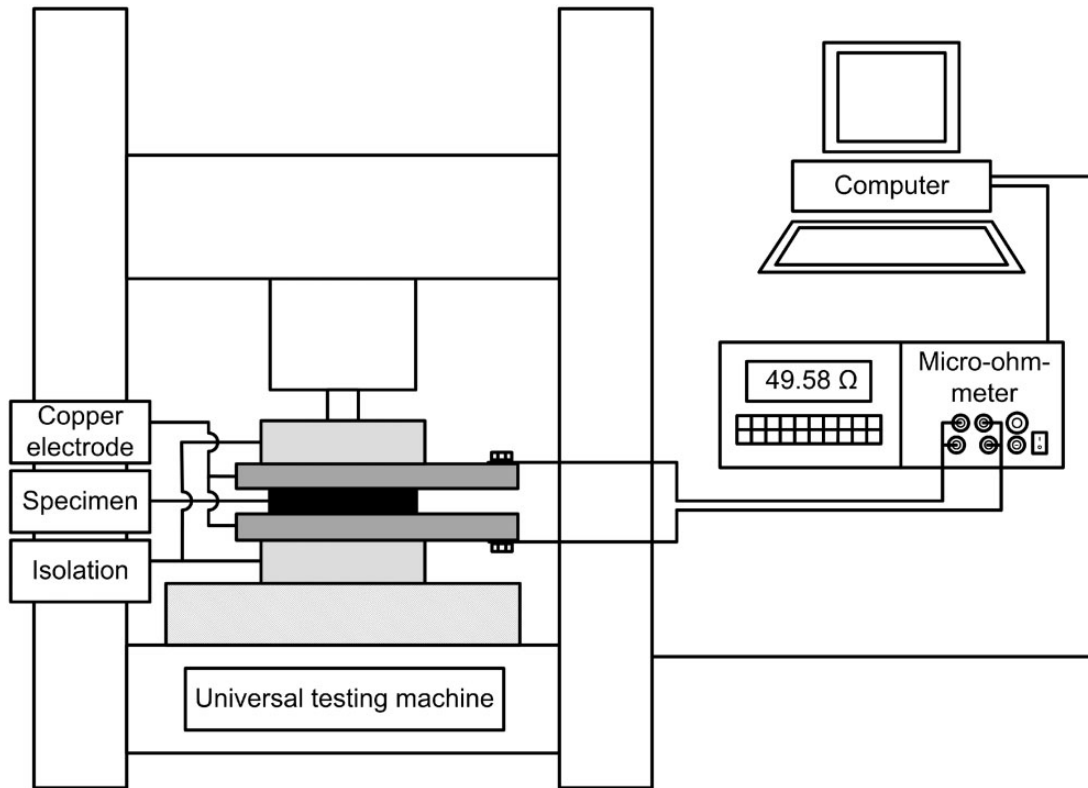


**Figure 3.** Schematic view of the test rig for determining the electrical conductivity of the carbon composite samples along their three main axes.

shear strength of testing at elevated temperatures was also investigated. For this purpose, a Shimadzu TCE-N300 temperature chamber came into play, in which the samples were first heated to 80 °C and held at this temperature for an hour before being tested, the procedure being repeated at 120 °C. For each type of composite and for each test temperature, five samples were produced and tested. The authors would like to point out that because of the small span-to-thickness ratio, the influence of the supports will cause a more complex stress distribution which is not well described with (1). For this reason, the numbers should be compared only relatively to each other.

The Mode I and Mode II interlaminar energy release rates (GIc and GIIC) were determined according to the DIN standards 6033 and 6034, respectively. All samples were tested using a Shimadzu AG-X 10 kN universal testing machine with a constant crosshead speed of 10 mm/min for GIc and 1 mm/min for GIIC. The samples were 110 mm long by 25 mm wide. For each distinct type of composite, five samples were produced and tested.

## Results and discussion

The primary goal of this study was to investigate how mixing various nano-based additives with PA12 affects

fracture toughness, interlaminar shear strength ILSS, the mode I and II energy release rates as well as the electrical conductivity of CFRP. It was the general intention to find out how high the nanoparticle content needs to be in order to obtain a significant improvement in the electrical conductivity along the three main axes of the laminate. Besides this the question was whether adding these particles was necessary at all, given that adding them increases the cost of producing the CFRP components.

For this purpose, the electrical conductivity of the various modified PA12 powders was to be examined, after which building them into the interlaminar layer should demonstrate how effectively they influence the electrical conductivity and the mechanical properties of the CFRP. Table 1 compares the thickness and the fibre volume content of all the samples tested (the thickness given is the average for the five samples).

### *The electrical conductivity of additive enhanced PA12*

Figure 4 shows how the electrical conductivity of different PA12 compounds depends on the compression of the powder. Each point represents the mean of the five sample values, the scatter about the mean being no more than 5%. Most noteworthy is the logarithmic

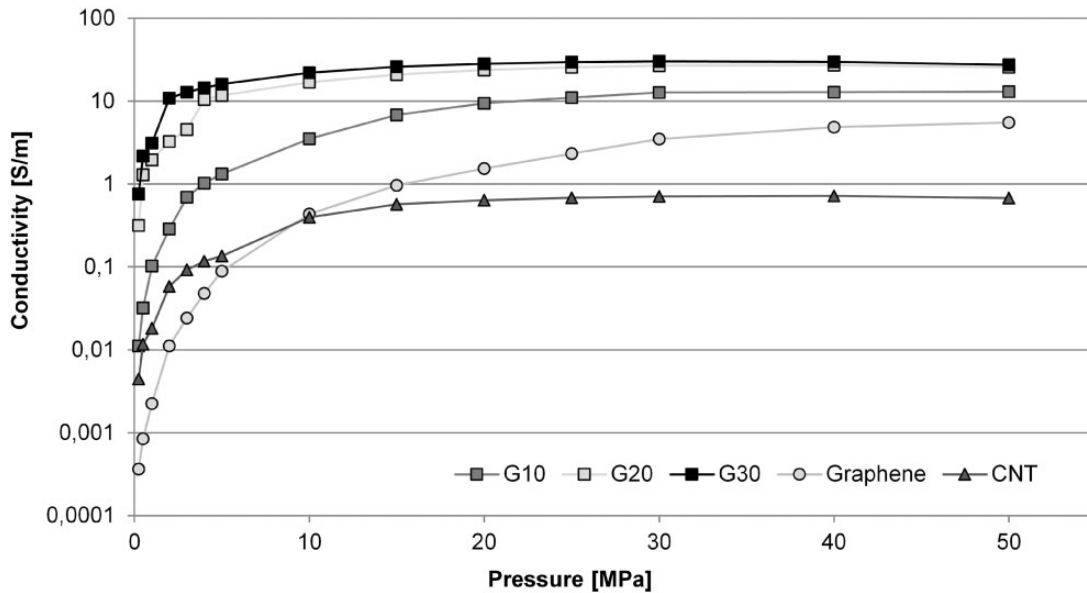


Figure 4. The effect of compression on the electrical conductivity of additive-enhanced PA12.

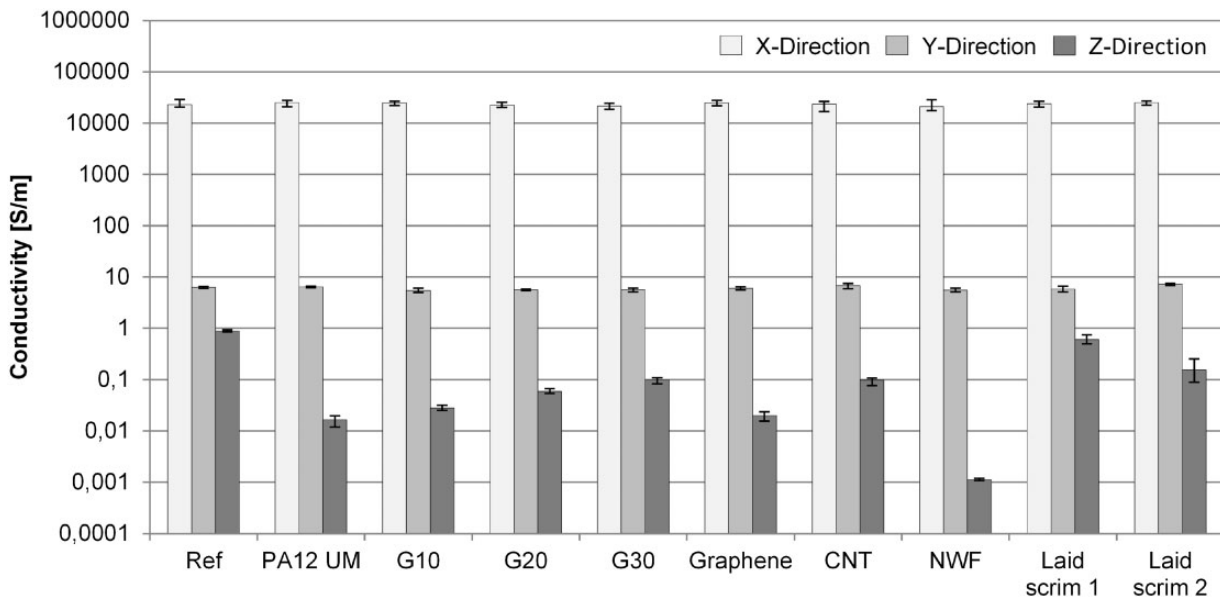


Figure 5. Electrical conductivities of the composites in the three main directions X, Y and Z.

evolution of conductivity with compression. It is clear that in all cases, increasing compression tends to raise the conductivity, this tendency being particularly marked in the case of graphene, whose conductivity increases by about four orders of magnitude between 0.25 MPa and 50 MPa. For all the materials, the greatest increase in conductivity occurs between 0.25 MPa and 10 MPa.

It can also be seen that whatever the pressure may be, it is always the graphite-modified samples that have the highest electrical conductivity. For all these, the

steepest increase takes place below 10 MPa, the rate of increase falling off rapidly above 20 MPa. Below 10 MPa, CNT has higher conductivity than graphene, but from that point on its slope falls off to finish below 1 S/m.

#### The electrical conductivity of the composites

Figure 5 shows the electrical conductivity of the tested composites in the directions of the three main axes. The test current was 1 A in the fibre direction Y and

thickness direction  $Z$ , and 0.1 A in the  $Y$ -direction at right angles to the fibre direction in the plane of the sample. It should be noted that the scale of the  $Y$ -axis is logarithmic: the resistances in the three directions differ by orders of magnitude.

These results show that none of the additives – i.e. thermoplasts with or without particles – have any significant effect on the conductivity in the  $X$ -direction or in the  $Y$ -direction, the variation within the respective range being less than  $\pm 10\%$ . One can discern no clear trend in favour of this or that combination of materials. Thus conductivity in these two directions is not reduced by the PA12, nor is it improved by any of the additives. The modification is unsuccessful in the  $X$ -direction due to the inherently high conductivity of carbon fibres. On the other hand, some modification of the conductivity in the  $Y$ -direction by means of a modified PA12 powder may be practicable. This, however, is hindered by the discrete distribution of the various PA12's due to their powder form. A flat insert, for example of foil, or a coating could remedy this.<sup>25</sup>

The conductivity through the thickness (the  $Z$ -direction) of the reference sample is 85% lower than that in the  $Y$ -direction, while the samples with modified PA12 show a further fall-off in electrical conductivity compared with that of the reference sample. Comparing the results for the three graphite-containing samples it is noticeable that conductivity improves with increasing graphite content: 20% graphite content gives 250% better conductivity than unmodified PA12, and 30% even 500% better. All the same, the conductivity still remains an order of magnitude lower than that of the reference sample.

In the pressure tests of the dry powder, the conductivity of the CNT-modified samples is more than an order of magnitude lower than that of the graphite-modified samples; this difference is, however, not to be seen in the results for the composite samples. This contradiction is due to the different particle shapes of the powder used. Figure 6 shows photomicrographs of some of the samples. It can be seen that the CNT particles are distinctly bigger in diameter than those, for example, of graphite. The larger CNT particles ensure better connections with the individual fibre layers and hence improved conductivity. Thus, the sample with PA12 and 20% CNT has the same  $Z$ -conductivity as that with PA12 and 30% graphite. Graphene in the interlaminar layer also increases  $Z$ -conductivity: it is 20% higher than that of the sample with unmodified PA12. Furthermore, an influencing of the results by a possible orientation of the additives in the particles is not to be expected.

NWF, on the other hand, leads to a clear reduction in  $Z$ -conductivity: it is three orders of magnitude less than that of the reference sample. This can be traced back to a clear increase in the thickness of the interlaminar layer. Furthermore, it has been shown that

during the curing cycle of RTM6, the PA12 only begins to melt when the resin is already solidified, making a reduction in layer thickness impossible.<sup>3</sup> In contrast, the presence of a lattice in the interlaminar layer affects conductivity but slightly: Laid scrim 1 reduces conductivity by only 31% relative to that of the reference sample, the lowest reduction of all the tested samples. This notable distinction in the performance of laid scrim is caused by the favourable interaction between the carbon fibres and the thermoplastic yarn, the yarn causing a local increase in the fibre volume content. As can be seen in Figure 7, a resin-rich layer forms around the yarn, but the effect is localized to the zone immediately next to the yarn, and away from this zone the thickness of the interlaminar layer is the same as that of the reference sample. This effect is referred to as interlocking. The figure shows a partial section in one direction. The section is of course the same in the direction at right angles, so there are areas between the melted yarns which are not modified by the PA12, which in aggregate form the greater part of the interlaminar layer. Thus, most of this layer is unimpaired, and this shows itself in the relatively slight reduction in electrical conductivity in the  $Z$ -direction of the sample. On the other hand, the  $Z$ -conductivity of Laid scrim 2 is significantly lower because it has a greater proportion of yarn in the interlaminar layer than that of Laid scrim 1.

### Compressive strength after Impact CAI

In the CAI test results, interest centred on the reduction in the area of delamination as well as on the residual compressive strength. The basis for comparison is the result for the reference samples that were produced without the thermoplastic inlayer. Figure 8 shows clearly that all the additives reduce not only the area of delamination but also the scatter of the results for the five samples about their mean value. It is also apparent that there are only slight differences between the results for the various additives and the result for unmodified PA12. Thus, the samples modified with graphene show 13% more delamination than those with PA12 UM, while using NWF and Laid scrim 2 reduces the delaminated area by 17%. In contrast, the samples with CNT, G30 and Laid scrim 1 all show more than 50% increase in area of delamination compared with that for PA12 UM.

A similar pattern can be seen also in the results for residual compressive strength (Figure 9). The increase in strength is much the same for all the variants. Once again it is apparent that of all the modifications to the PA12, that with CNT brings the least advantage, with only 18% more than the reference result, and even 14% below that for unmodified PA12. The Laid scrim 1 value

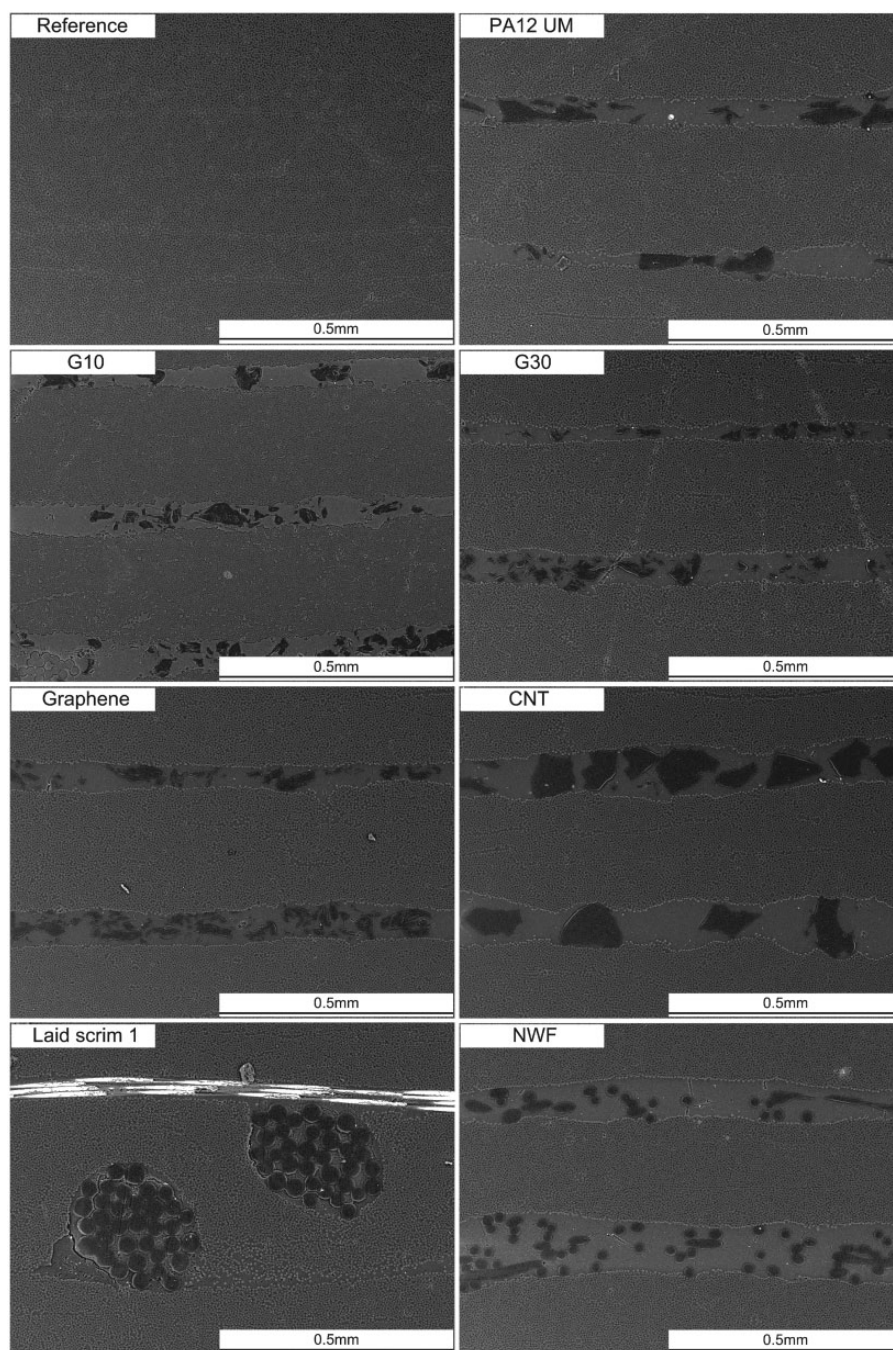


**Figure 6.** Photomicrographs of the tested samples, after etching for 20 minutes with 16% hydrochloric acid (HCl).

is 14% less than the reference. The Graphene and G10 values on the other hand are more than 30% higher than the reference, corresponding to the results of unmodified PA12. The corresponding values are only slightly lower for the other modifications to the PA12.

#### *Interlaminar shear strength ILSS*

Figure 10 gives the results of the ILSS tests. It can be seen that the reference samples show little change in

shear strength with increasing temperature, whereas for all the samples with PA12, in no matter what form, it falls off as the temperature increases. This can be explained by the temperature-dependency of the Young's modulus of PA12: as the temperature rises from 20 °C to 120 °C, it falls by about 80%.<sup>25</sup> The resin layer, with its high shear strength, is interrupted by the thermoplastic, which becomes less stiff as the temperature rises, so leading to a fall-off in the shear strength of the composite. This fall-off amounts



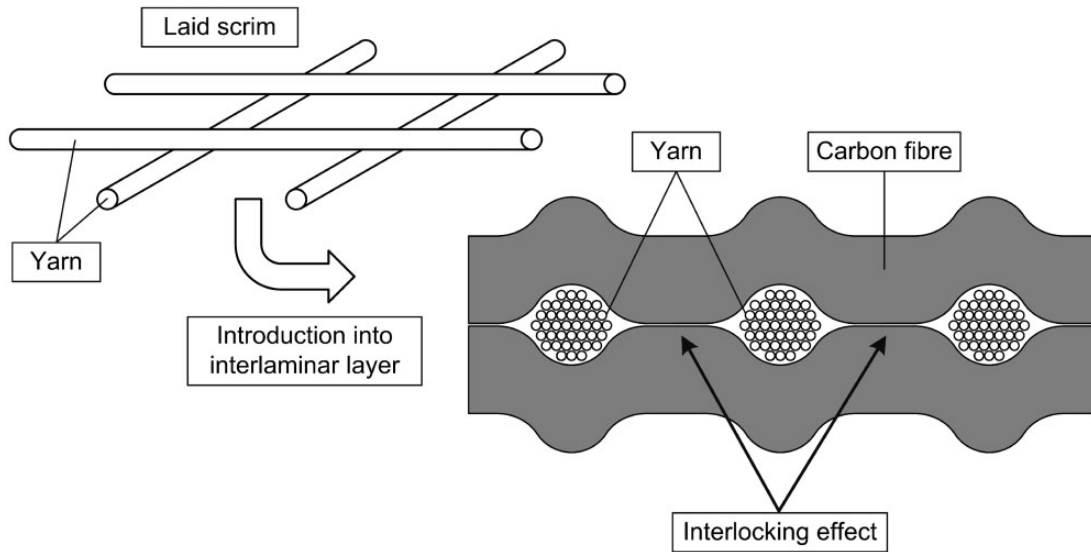


**Figure 7.** Effect of the laid scrim on the thickness of the interlaminar layer.

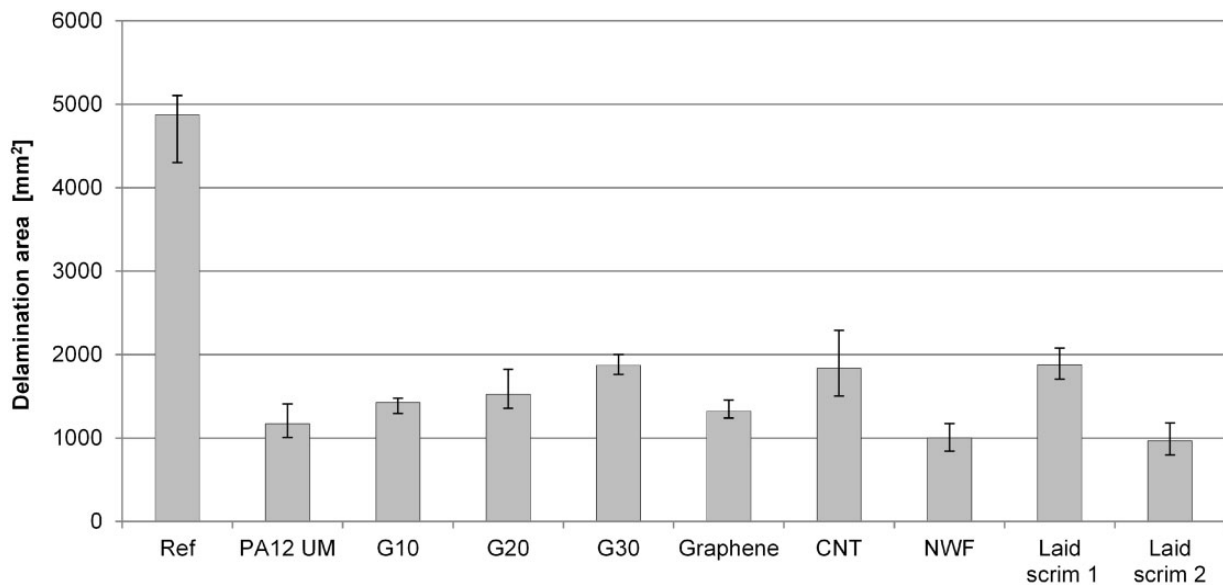


**Figure 8.** Area of delamination in the CAI tests.

to about 17% for the unmodified PA12 samples, and to 12–28% for the modified PA12 samples. With a reduction of only 12%, it is the CNT-modified samples that react least strongly to the rise in temperature. It can hence be concluded that additives do not completely compensate for the fall-off in the Young’s modulus of PA12 with increasing temperature.

**Mode I interlaminar energy release rate  $G_{Ic}$**

Figure 11 shows the Mode I energy release rates of the test samples. As can be seen, the  $G_{Ic}$  values clearly improve with the addition of unmodified PA12 powder. PA12

UM, NWF, and Laid scrim all very effectively increase the energy release rate, in particular Laid scrim 1, in which the PA12 yarn in the interlaminar layer is highly effective in diverting cracks and so increasing the energy release rate by 75% over that of the reference samples.

It can be seen on the other hand that modifying PA12 with graphite has a negative effect on the energy release rate. Moreover, raising the graphite content from 10% to 30% causes a 14% drop in  $G_{Ic}$  value, so raising the graphite content further reduces the strength of the interlaminar layer. Figure 12 shows the fracture patterns of some of the samples, and as can be seen, their surface structures differ substantially. Laid scrim 1 has a smooth

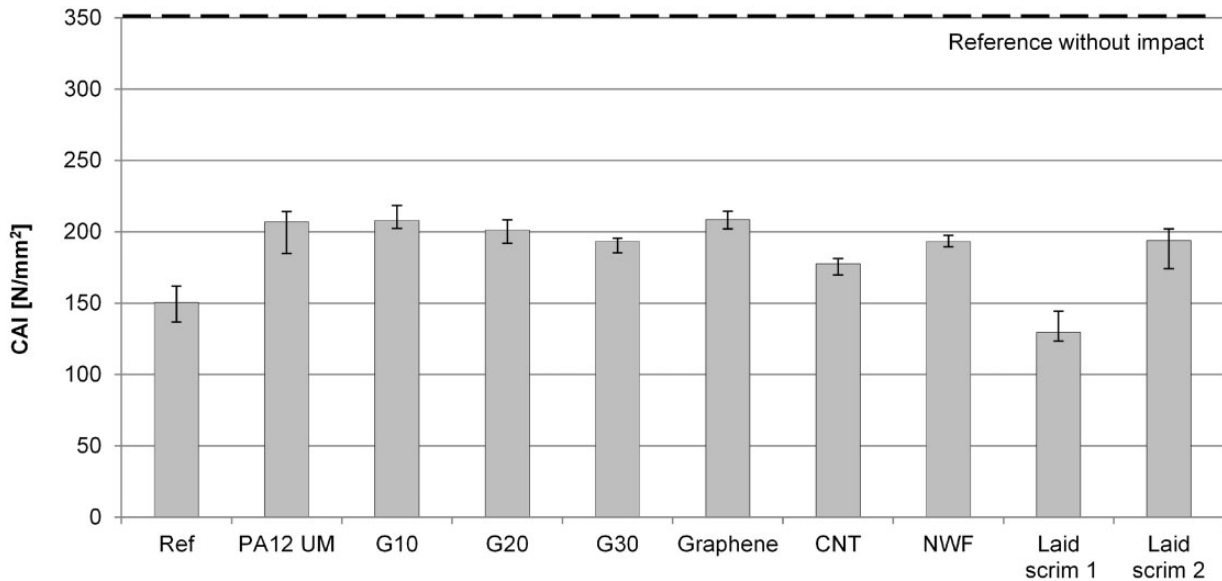


Figure 9. Residual compressive strength in the CAI tests.

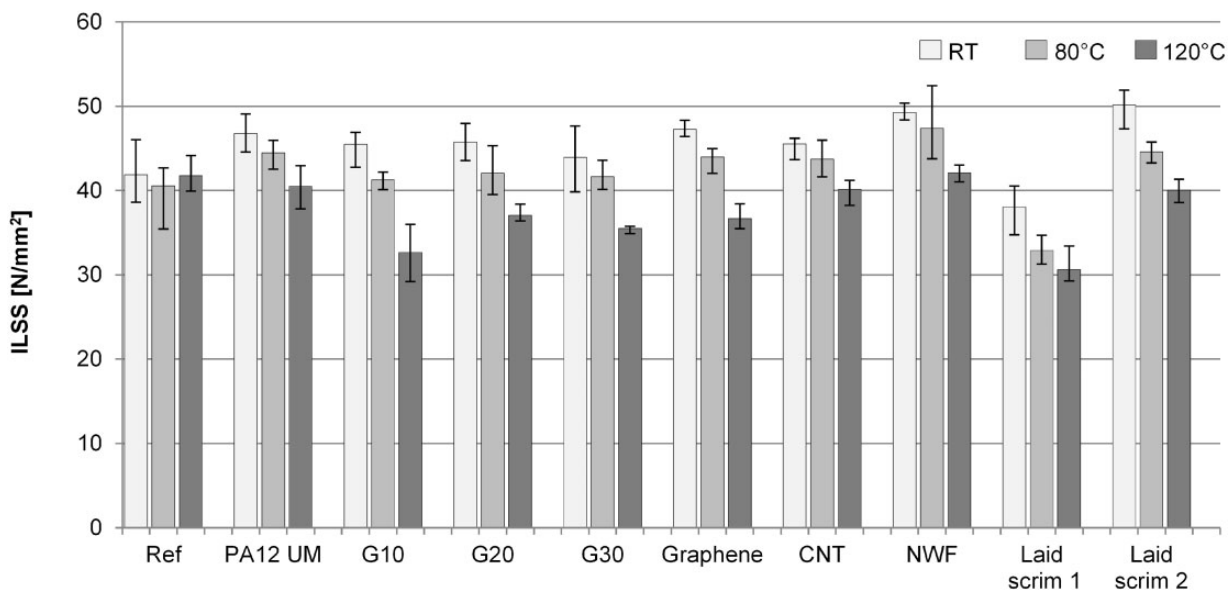


Figure 10. Interlaminar shear strength at various test temperatures.

surface interrupted by the PA12 yarns. In contrast, CNT and PA12 have a clearly defined structure with larger flat rupture surfaces in the resin-rich layer. The effect of this behaviour on the energy release rate is, however, minimal, and mixing the PA12 with additives does not have a positive effect on the interlaminar energy release rate.

#### Mode II interlaminar energy release rate $G_{IIc}$

Figure 13 shows the Mode II energy release rates, and what immediately stands out is that the most effective

modification is the use of NWF in the interlaminar layer, which increases fracture toughness by over 300% relative to that of the reference samples. Apart from this, the energy release rate pattern for the samples with unmodified and modified PA12 powder is very similar to that in the  $G_{Ic}$  tests. The  $G_{IIc}$  values for the samples with modified PA12 are significantly higher than the reference value. Both graphene and CNT show a more than 200% increase relative to the reference. Increasing the graphite content, however, causes the energy release rate to fall by 22% as the graphite content rises from 10% to 30%. Introducing

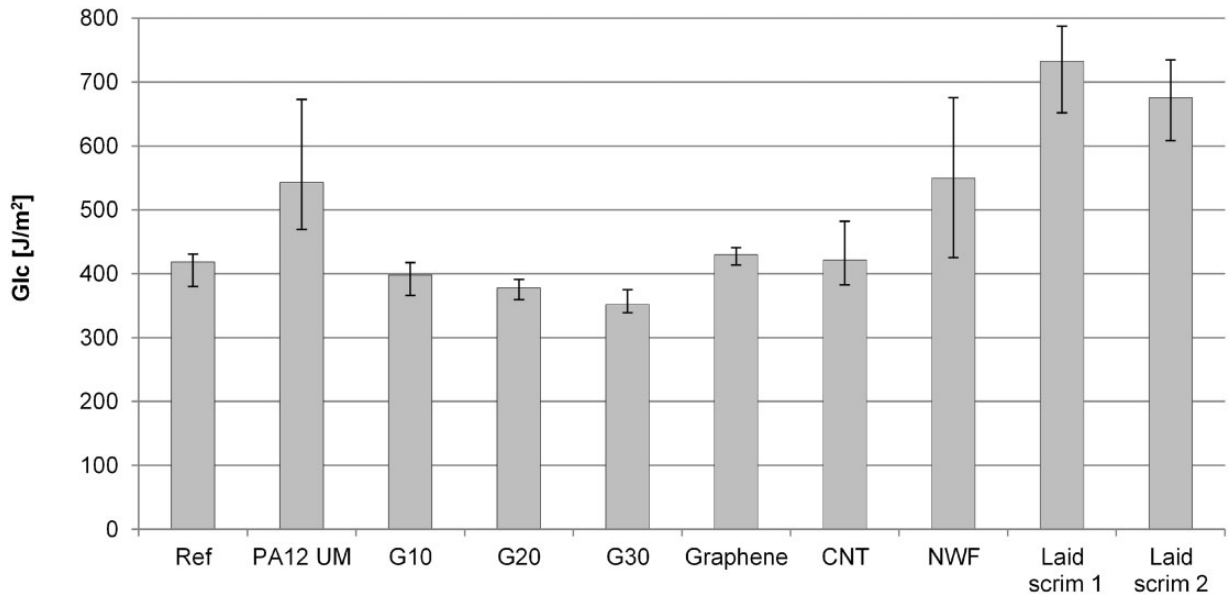


Figure 11. Mode I Interlaminar energy release rates.

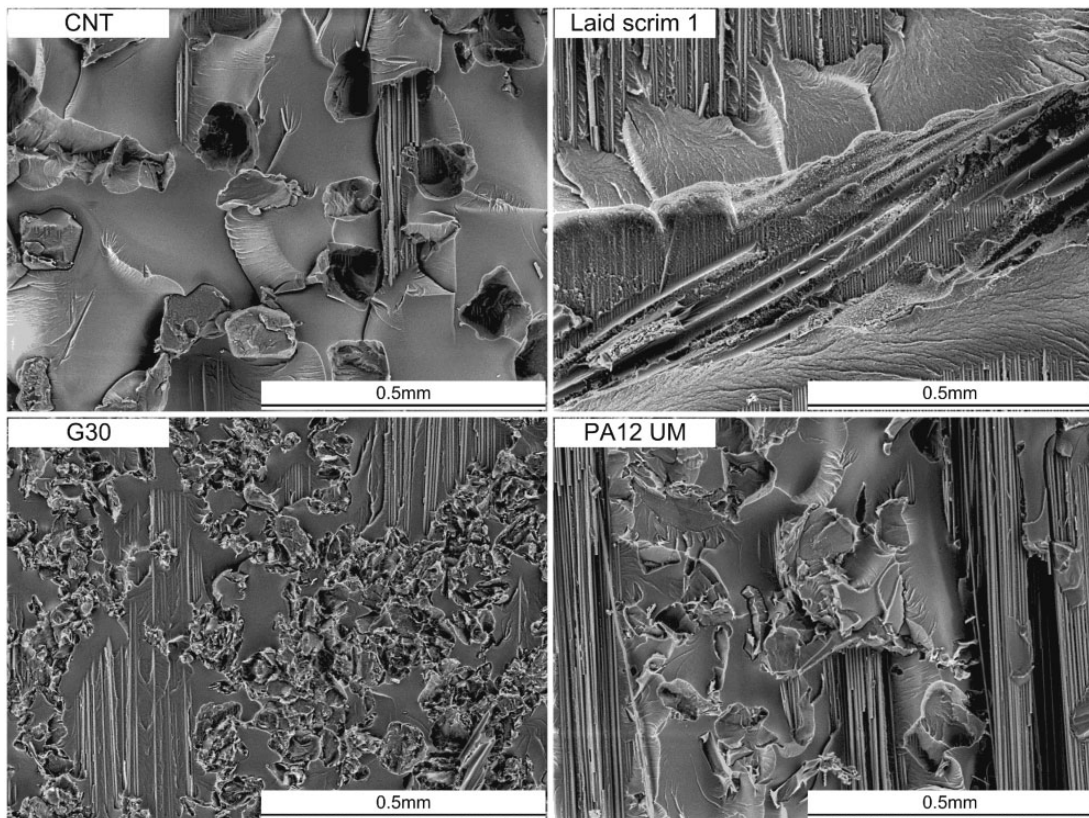


Figure 12. Surface textures after Glc testing.

unmodified PA12 into the interlaminar layer improves fracture toughness by 180% relative to the reference. Its performance relative to that of graphene- and CNT-modified PA12 does not match that seen in the Glc

tests, however, in which it is clearly superior. So the conclusion here is that adding graphene or CNT to PA12 brings no advantage as regards the shear stress-dependent energy release rate.

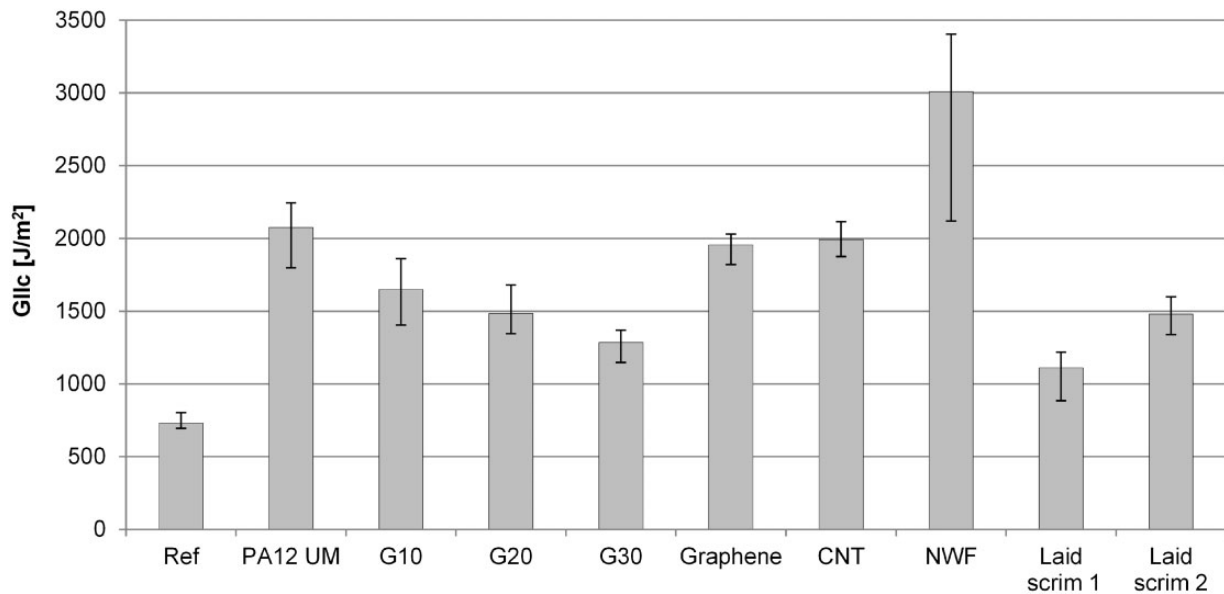


Figure 13. Mode II Interlaminar energy release rates.

## Conclusions

This study investigated the influence of modified PA12 powder as well as various PA12 inserts on the electrical conductivity and fracture toughness behaviour of carbon/epoxy resin composites. The tests showed first of all that building PA12 into the interlaminar layer led to a fall in the electrical conductivity through the thickness of the composite (the Z-direction). Mixing the electrical conductive additives graphite, graphene and CNT into the PA12 remedied this to some extent. This, however, necessitated high concentrations of the additives which in turn negatively affected the fracture toughness. In general, the relatively high electrical conductivity of the modified PA12 powder does not carry over into an equivalent improvement in the electrical conductivity of the composites. When a discrete insert was used, in this case the laid scrim, the electrical conductivity dropped much less due to the interlocking effect. This was because with laid scrim, a large part of the interlaminar layer is not actually covered with thermoplastic. Regarding the fracture toughness behaviour of the modified CFRP composites, no superior effect could be found by the addition of the electrically conductive additive to PA12.

## Outlook

In general, the results suggest that for the laid scrim, an ideal combination of yarn size, yarn spacing and the resulting specific weight could not be determined within this work. However, the laid scrim shows advantages over continuous inlayers due to its mechanical and electrical properties. Moreover, an additional and

expensive modification of the PA12 with electrically conductive additive is not necessary. So, further developments of the material can allow applications of these inlayers in the aviation.

## Acknowledgements

The authors wish to thank: EMS-CHEMIE AG for providing the polymers; BAFATEX Bellingroth GmbH & Co. KG for providing the laid scrims; SAERTEX GmbH & Co. KG for providing the carbon fibre.

## Conflict of interest

None declared.

## Funding

This work was supported by Werner-Steiger-Stiftung.

## References

1. Ultracki LA. *Polymer alloys and blends: thermodynamics and rheology*. Munich: Hanser Publishers, 1989.
2. Cantwell WJ, Curtis P and Morton J. An assessment of the impact performance of CFRP reinforced with high-strain carbon fibres. *Compos Sci Technol* 1986; 25: 133–148.
3. Arnold M, Henne M, Bender K, et al. The influence of various kinds of PA12 interlayer on the interlaminar toughness of carbon fibre-reinforced epoxy composites. *Polym Compos*. Epub ahead of print 18 April 2014. DOI: 10.1002/pc.23029.
4. Tsotsis TK. Interlayer toughening of composite materials. *Polym Compos* 2003; 30: 70–84.
5. Uman MA and Rakov VA. The interaction of lightning with airborne vehicles. *Prog Aerosp Sci* 2003; 39: 61–81.

6. Gou J, Tang Y, Liang F, et al. Carbon nanofibre paper for lightning strike protection of composite materials. *Compos Part B* 2009; 41: 192–198.
7. Feraboli P and Miller M. Damage resistance and tolerance of carbon/epoxy composite coupons subjected to simulated lightning strike. *Compos Part A* 2009; 40: 954–967.
8. Uman MA and Rakov VA. *Lightning: physics and effects*. Cambridge: Cambridge University Press, 2006.
9. Uman MA. *The art and science of lightning protection*. Cambridge: Cambridge University Press, 2010.
10. Garcia EJ, Wardle BL, Hart AJ, et al. Fabrication and multifunctional properties of a hybrid laminate with aligned carbon nanotubes grown *In Situ*. *Compos Sci Technol* 2008; 68: 2034–2041.
11. Kim HS and Hahn HT. Graphite fiber composites inter-layered with single-walled carbon nanotubes. *J Compos Mater* 2011; 45: 1109–1120.
12. Wang H and Siow KS. Measurement of  $T_g$  in epoxy resins by DSC—effects of residual stress. *Polym Eng Sci* 1999; 39: 422–429.
13. Niu MCY. *Composite airframe structures*. Hong Kong: Conmilit Press Ltd, 1993.
14. Stephenes CO. Advanced composite vertical stabilizer for DC-10 transport aircraft. Report no. NASA-CR-172780, National Aeronautics and Space Administration (NASA), USA, June 1978.
15. Sandifer JP, Denny A and Wood MA. Fuel containment and damage tolerance in large composite primary aircraft structures. Phase 2: testing. Report no. NASA-CR-172519, National Aeronautics and Space Administration (NASA), USA, March 1985.
16. Mulazimoglu H and Haylock L. Recent developments in techniques to minimize lightning current arcing between fasteners and composite structure. *SAE Int J Aerosp* 2010; 2: 232–238.
17. Guo M and Yi X. The production of tough, electrically conductive carbon fibre composite laminates for use in airframes. *Carbon* 2013; 58: 241–244.
18. Valera MTB, Pons F and Woelcken PC. Nanotechnology for advanced composite airframes. In: *Proceedings of the 8th SAMPE Europe international technical conference*, Wuppertal, Germany, 11–12 September 2013, pp.176–183.
19. Marinho B, Ghislandi M, Tkalya E, et al. Electrical conductivity of compacts of graphene, multi-wall carbon nanotubes, carbon black, and graphite powder. *Powder Technol* 2012; 221: 351–358.
20. Celzard A, Marêche JF, Payot F, et al. Electrical conductivity of carbonaceous powders. *Carbon* 2002; 40: 2801–2815.
21. Kim BC, Park SW and Lee DG. Fracture toughness of the nano-particle reinforced epoxy composite. *Compos Struct* 2008; 86: 69–77.
22. Cinquin J, Heinrich C and Balland E. Volume electrical conductivity measurement on organic composite materials. In: *Proceedings of the 8th SAMPE Europe international technical conference*, Wuppertal, Germany, 11–12 September 2013, pp.192–202.
23. Todoroki A and Yoshida J. Electrical resistance change of unidirectional CFRP due to applied load. *JSME Int J A-Solid Mater* 2004; 47: 357–364.
24. Reia da Costa EF, Skordos AA, Partridge IK, et al. RTM processing and electrical performance of carbon nanotube modified epoxy/fibre composites. *Compos Part A* 2012; 43: 593–602.
25. Zhang B, Patlolla VR, Chiao D, et al. Galvanic corrosion of Al/Cu meshes with carbon fibers and graphene and ITO-based nanocomposite coatings as alternative approaches for lightning strikes. *Int J Adv Manuf Tech* 2013; 67: 1317–1323.
26. EMS-CHEMIE AG, Polyamide 12 brochure, [www.emsgrivory.com/fileadmin/ems-grivory/documents/brochures/Grilamid-L-PA12\\_3001\\_en.pdf](http://www.emsgrivory.com/fileadmin/ems-grivory/documents/brochures/Grilamid-L-PA12_3001_en.pdf) (accessed 21 October 2014).